Thomas Schneider von Deimling · Hermann Held
Andrey Ganopolski · Stefan Rahmstorf

Climate sensitivity estimated from ensemble simulations of glacial climate

Abstract The concentration of greenhouse gases (GHGs) in the atmosphere continues to rise, hence estimating the climate system's sensitivity to changes in GHG concentration is of vital importance. Uncertainty in *climate sensitivity* is a main source of uncertainty in projections of future climate change. Here we present a new approach for constraining this key uncertainty by combining ensemble simulations of the last glacial maximum (LGM) with paleo-data. For this purpose we used a climate model of intermediate complexity to perform a large set of equilibrium runs for (1) pre-industrial boundary conditions, (2) doubled CO_2 concentrations, and (3) a complete set of glacial forcings (including dust and vegetation changes). Using proxy-data from the LGM at low and high latitudes we constrain the set of realistic model versions and thus climate sensitivity. We show that irrespective of uncertainties in model parameters and feedback strengths, in our model a close link exists between the simulated warming due to a doubling of CO_2, and the cooling obtained for the LGM. Our results agree with recent studies that annual mean data-constraints from present day climate prove to not rule out climate sensitivities above the widely assumed sensitivity range of 1.5–4.5°C (Houghton et al. 2001). Based on our inferred close relationship between past and future temperature evolution, our study suggests that paleo-climatic data can help to reduce uncertainty in future climate projections. Our inferred uncertainty range for climate sensitivity, constrained by paleo-data, is 1.2–4.3°C and thus almost identical to the IPCC estimate. When additionally accounting for potential structural uncertainties inferred from other models the upper limit increases by about 1°C.

Abbreviations ΔT_{2x}: Climate sensitivity · TCR: Transient climate response · GCM: General circulations model · IPCC: Intergovernmental panel on climate change · LGM: Last glacial maximum · GHG: Greenhouse gas · CO_2: Carbon dioxide · SST: Sea surface temperatures · SAT: Surface air temperature

T. Schneider von Deimling (✉) · H. Held · A. Ganopolski
S. Rahmstorf
Potsdam Institute for Climate Impact Research (PIK),
P.O. Box 60 12 03, 14412, Potsdam, Germany
E-mail: schneider@pik-potsdam.de
Tel.: +49-331-2882630
Fax: +49-331-2882640
E-mail: held@pik-potsdam.de

1 Introduction

The "climate sensitivity" ΔT_{2x} provides the most important measure for the sensitivity of the climate system to changing atmospheric greenhouse gas (GHG) concentrations. It is defined as the global-mean equilibrium surface air warming following a doubling of atmospheric CO_2 concentration. Two principal ways can be pursued to determine ΔT_{2x}.

The first ("bottom–up") approach is based on a quantitative understanding of the physical mechanisms: the direct changes in radiation balance and associated positive and negative feedbacks, such as water vapour, cloud, albedo and lapse rate (vertical temperature profile) feedbacks, which can be calculated by models. Although the underlying processes can to some extent be validated by observations of modern climate, there is still considerable uncertainty in the strength of these feedbacks, most notably the cloud feedback. Hence, it has not been possible on this basis to reduce the range of uncertainty of ΔT_{2x} since the 1970s, when it was first estimated as 1.5–4.5°C (Charney 1979). Recent studies with comprehensive climate models (Stainforth et al. 2005) have shown that it is possible to construct model versions with climate sensitivities exceeding 10°C, which are consistent with annual mean data of modern day climate characteristics. But

when considering additional data information, such as the annual cycle, it seems quite likely that those models will show to be inconsistent with climatology.

The second ("top–down") approach is to analyse how climate has changed in the past when GHG concentrations have changed. Several studies have attempted this based on data for the last glacial maximum (LGM; Hoffert and Covey 1992; Hansen et al. 1993; Covey et al. 1996). One of the difficulties here is that there is no direct past analogue for a future large increase in GHG concentrations, with all other factors influencing climate being the same as today. Generally, several climate forcings have changed simultaneously, making it difficult to isolate the effect of GHGs, although this can be tried by using multivariate analysis on long time series (Lorius et al. 1990). Also, the mean climate state was different in the past (e.g. much colder during Glacials), hence the strength of feedbacks such as albedo or water vapour feedback probably differed as well.

Here, we apply a "third way" of deriving ΔT_{2x}, based on systematically combining our understanding of the physics with data from past climate evolution, including uncertainty in both factors. The basic idea is to generate an ensemble of many climate model versions with different parameters and hence different strengths of relevant feedbacks, in order to span the current uncertainty in physical understanding, and then use observational or proxy-data to constrain which subset of these models (and hence what range of ΔT_{2x}) is compatible with pre-industrial climate and past climate evolution.

This method has previously been applied to the 20th Century climate change, i.e. the period of anthropogenic increase in CO_2 concentration (Forest et al. 2002; Knutti et al. 2002). The conclusion from these ensemble simulations is that the anthropogenic warming signal is too weak to effectively constrain ΔT_{2x}, due to uncertainty in the radiative forcing over the industrial period, in the observational data and in the rate of ocean heat-uptake. Further studies, which also focus on the historical warming temperature signal, fail as well in effectively constraining the ΔT_{2x} range, particularly the upper bound (Andronova and Schlesinger 2001; Gregory et al. 2002); i.e. within current physics uncertainty it is possible to construct models with a very high ΔT_{2x} ($\sim$7°C), and such models are not ruled out by the relatively small 20th Century warming if aerosol shading was large over this period.

Here we apply this third method to the climate of the LGM ($\sim$21 kyr BP). This period represents one of the largest deviations from present climate in recent geologic history, with estimates for global cooling from simulations (Ganopolski et al. 1998; Kitoh et al. 2001; Hewitt et al. 2003; Shin et al. 2003) ranging from 4 to 6°C.[1]

The LGM is promising for constraining ΔT_{2x} since (1) the GHG changes are large, (2) the climate signal is large, (3) the cold climate persisted for millennia, so is in near-equilibrium, (4) the forcing and response are reasonably well known, and (5) successful simulations of glacial climate are available. In view of constraining high climate sensitivities, uncertainty in maximum negative forcing contributions from aerosols (Anderson et al. 2003) affects—for the LGM—the lower, not upper limit of the sensitivity range (unlike for modern climate constraints).

While some authors have discussed ΔT_{2x} in the context of a single LGM simulation (Hewitt and Mitchell 1997; Broccoli 2000), (to best of our knowledge) this study represents the first estimate of ΔT_{2x} that is based on an ensemble of fully coupled simulations for the LGM climate. An ensemble study with an atmospheric general circulation model (GCM) coupled to a slab ocean recently has been performed for PMIP-2 boundary conditions (Annan et al. 2005). We accounted for a complete set of the main radiative forcing changes between the pre-industrial and glacial climate, including dust concentration and vegetation changes, which crucially contribute to the cooling but which have been neglected in previous simulations with coupled climate models (Kitoh et al. 2001; Hewitt et al. 2003; Shin et al. 2003).

Our study shows that the LGM climate is likely to constrain the upper end of the ΔT_{2x} range. At least within the range of processes captured by our model—and provided that the simulated relationship between LGM cooling and CO_2 warming covered in our ensemble does not strongly differ from that simulated by different GCMs (see Section 5)—a high ΔT_{2x} (larger than $\sim$5.3°C) cannot be reconciled with most recent paleo-proxy estimates of cooling between the LGM and pre-industrial climate.

2 Methods

Using the CLIMBER-2 model of intermediate complexity (see Section 3) we performed a large set of ensemble simulations for pre-industrial, doubled CO_2 concentration and glacial boundary conditions (Table 1). For all simulations we perturbed the same set of 11 model parameters, which mainly affect the model-inherent feedback strengths, to derive a set of model versions with differing climate sensitivities.

2.1 Sampling strategy

We selected those parameters of CLIMBER-2 that are most influential on the model-intrinsic climate sensitivity (for details on our choice, see Appendix 7.3). As (Forest et al. 2002; Knutti et al. 2002) have done for their parameter choices, we explored the—in our case—11-dimensional parameter space according to a Monte Carlo scheme. First, for any of

---

[1] It should be noted that those LGM simulations do not account for the forcing effects of dust and vegetation changes. If these forcings are included as further boundary conditions an additional global surface air temperature (SAT) cooling of about 1.5 to 2°C can be expected (Schneider von Deimling et al., in preparation).

Table 1 Overview of model simulations and applied boundary conditions

	Year	Forcing	Parameter setting
SIM_2CO$_2$	1–3,500	Pre-industrial boundary conditions	Ensemble-1
	3,501–3,570	1% CO$_2$ increase (280–560 ppm)	
	3,571–6,500	Constant CO$_2$ (560 ppm)	
SIM_LGM	1–3,500	LGM ice sheets, CO$_2$, dust, solar insolation, vegetation	Ensemble-1
SIM_LGM0.5	1–3,500	Same as SIM_LGM, but only 50% dust forcing	Ensemble-1
SIM_CO$_2$_LGM	1–3,500	Pre-industrial conditions, but CO$_2$ = 180 ppm	Ensemble-2
SIM_abCO$_2$_LGM	1–3,500	Same as SIM_LGM, but CO$_2$ = 280 ppm	Ensemble-2
SIM_uncor	1–6,500	Same as SIM_2CO$_2$	Ensemble-3
SIM_uncor_LGM	1–3,500	Same as SIM_LGM	Ensemble-3

Ensemble-1: 1,000 parameter combinations, uniform-distributed, atmospheric parameters correlated. Ensemble-2: 500 parameter combinations, beta-distributed, correlations as in Ensemble-1. Ensemble-3: 5,000 (only pre-industrial consistent for SIM_uncor_LGM) parameter combinations, beta-distributed, uncorrelated

the 11 perturbed parameters we specified the interval for which the related parametrisation is meaningful according to the authors of the model. For our study, these authors represent the "experts" specifying "prior knowledge" according to the requirements of the Bayesian school. As no pronounced prior knowledge on correlations among the parameters was formulated, we follow the standard procedure and assume the prior distribution as uncorrelated among the parameters. Furthermore, as a continuous cut-off at the boundaries appears most natural we assume symmetrically beta-distributed (shape parameter of 1.75) (uncorrelated) parameters, hence, we conservatively assume a rather broad maximum of any marginal prior distribution. Finally, as we vary some parameters over orders of magnitude, we link the distributions to the logarithms of the parameters rather than the parameters themselves. We sampled this 11-dimensional, uncorrelated prior by a Latin-Hypercube scheme that represents an efficient variant of the Monte Carlo method. This sampling resulted in quite a narrow range of ΔT_{2x} (2.0–3.8°C) for an ensemble of 5,000 model runs (in the following termed "uncorrelated ensemble") even before applying any constraining information from observational data. While so far we have followed the standard procedure to initialise a rigorous Bayesian analysis, we also would like to ensure that the intervals we derive for ΔT_{2x} are predominantly a result of climate data constraints rather than the prior probability density chosen. In fact there is a long history of criticism of the fact that a result of a Bayesian scheme may strongly depend on the subjective choice of the prior distribution (for an overview, see Berger 1985 and Walley 1991, for a discussion in the context of climate sensitivity, see Frame et al. 2005). Hence, in the spirit of robust Bayesian statistics, we employ a second prior distribution that shall lead to much more conservative estimates of ΔT_{2x}. For that we modified the sampling scheme with the aim of a higher weighting of those parameter combinations that yield low and high ΔT_{2x}, thus increasing the sampling probability for the tails of the resulting distribution of ΔT_{2x}. We achieved a large range of ΔT_{2x} by positively

(negatively) correlating (factor ±0.9) all atmospheric parameters whose variations change ΔT_{2x} in the same (opposite) direction, e.g. we *systematically* (not randomly) combine positive and negative contributions to ΔT_{2x} of each parameter, and thus of the corresponding feedbacks.[2] In addition, we replaced the beta distribution by a uniform distribution, again stressing extreme values for ΔT_{2x}. We call the ensemble generated from this second prior the "correlated ensemble". The resulting frequency distribution looks rather uniform (thus gives approximately equal weight to all model versions with different climate sensitivities) in contrary to the more normal-like shape of ΔT_{2x}, derived from the uncorrelated ensemble (which peaks at 2.8°C).

2.2 Representation of dust forcing

The impact of dust probably represents the largest uncertainty in radiative forcing of LGM climate due to incomplete knowledge of its regional distribution and radiative properties (Claquin et al. 1998; Sokolik and Toon 1999). For the tropics, where the forcing by LGM dust is largest and postulated to be of the same order as of lowered CO$_2$ concentrations, it is very likely that the long-term climatic effect is a cooling (Harrison et al. 2001; Claquin et al. 2003).

Our climate model does not include a dust cycle, thus radiative effects of dust are prescribed as monthly top-of-the-atmosphere anomalies of the short-wave radiation, which have been calculated for modern and LGM boundary conditions, including dust concentration changes, from several ECHAM-5 (Stier et al. 2004) simulations (M. Werner, personal communication 2004).

Figure 1 shows the impact of dust forcing on the LGM cooling for the tropical oceans, which will serve as a focus area in our analysis (besides the region of

---

[2] The parameter correlations neither cause the inferred quasi-linear relation between ΔT_{2x} and the magnitude of LGM cooling (Fig. 5), nor systematic differences in the model results, as can be seen in Fig. 6.

Fig. 1 Additional tropical SST cooling through dust forcing. Shown is the difference in annual mean tropical SST cooling (globally averaged from 30°N to 30°S) between model versions which account for dust forcing [*green dots*: 100% dust forcing (SIM_LGM, see Table 1), *blue dots*: 50% dust forcing (SIM_LGM0.5)] and the same model versions without being forced by glacial dust. For a climate sensitivity of 3°C the additional cooling affected by LGM dust concentration changes is about 0.6°C (0.3°C) for 100% (50%) dust forcing
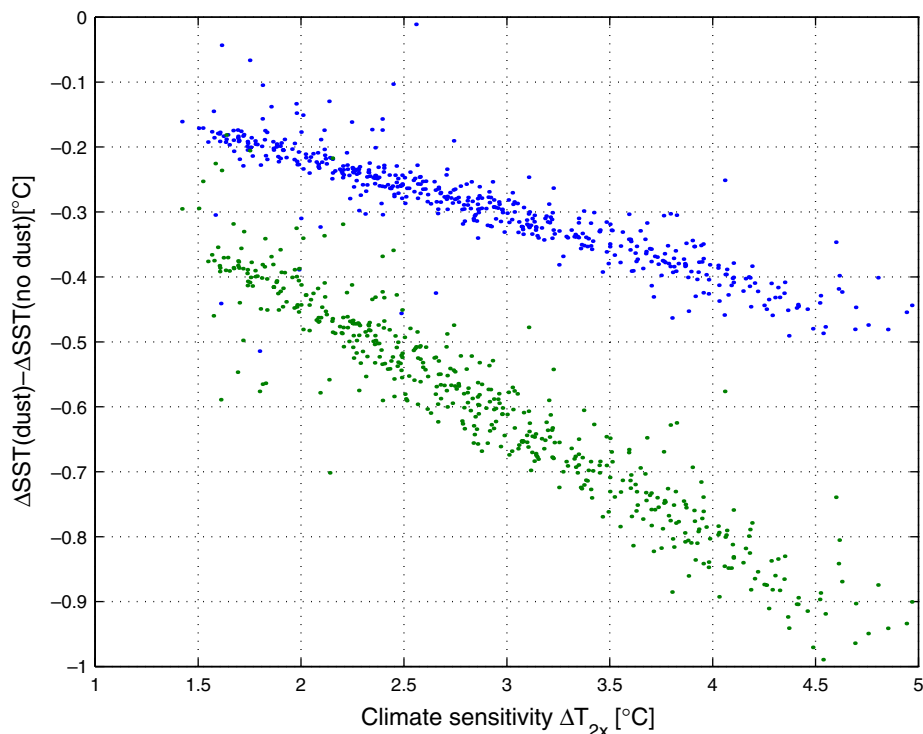
Eastern Antarctica) for the comparison of simulated and reconstructed glacial temperatures. The implementation of the radiative impact of glacial dust (100% scenario, Table 1) implies an additional global forcing of about -1.2 W/m^2 (-2.1 W/m^2 for the tropics, 0.3 W/m^2 for eastern Antarctica), which translates into an additional global SAT cooling of about 0.5 to 1.4°C [0.4–0.9°C for tropical sea surface temperatures (SSTs), 0.4–1.8°C for eastern Antarctica] for ΔT_{2x} between 1.5 and 4.5°C. The effect of a potential positive forcing caused by dust impact on snow albedo is small except in the area of high northern latitudes and thus is not crucial for our study.

3 Model simulations

We use a climate model of intermediate complexity (CLIMBER-2), consisting of a dynamical–statistical 2.5-dimensional atmosphere model (with parametrisations of the synoptic-scale activity), coupled without flux adjustments to a multi-basin, zonally averaged ocean model (Petoukhov et al. 2000). The simulated atmospheric and oceanic characteristics of the pre-industrial climate agree well with observational data (Petoukhov et al. 2000). Several sensitivity studies, e.g. of the model's response to a CO_2 concentration increase, qualitatively agree with results of GCMs (Ganopolski et al. 2001). Driven by natural and anthropogenic forcings, the model reproduces the temperature variations over the last millennium (Bauer et al. 2003). Simulated glacial climate shows many characteristics seen in proxy-data, both for the mean state (Ganopolski et al. 1998) and for

abrupt climate changes (Ganopolski and Rahmstorf 2001). An important requirement for this study is that the model simulates the key feedbacks that determine ΔT_{2x} (Colman 2003), namely the cloud, water vapour, albedo and lapse rate feedback. This is the case, with simulation of two cloud types, atmospheric lapse rate and tropopause height, a thermodynamic sea-ice and a land snow-cover module. In contrast to more simplified models, ΔT_{2x} is not a tuning parameter in our model, but arises from the model physics.

In our ensemble we considered uncertainties in 11 model parameters that strongly affect the above feedbacks. For those model versions consistent with present day climate, a comparison with GCM results (Colman 2003) shows that the realized spread in the individual feedbacks is comparable to the ranges covered by different GCMs, with the exception of water vapour feedback, which is at the lower end of the GCM range (with a relatively narrow spread) in our ensemble. Yet the range of combined water vapour and lapse rate feedbacks (these two are strongly anti-correlated in GCMs) overlaps with the lower half of the GCM spread and, more importantly, the sum of all feedbacks in our ensemble covers essentially the entire GCM range. Hence, in terms of the variation of climate feedbacks, our ensemble compares well with a sampling of more complex models.

Previous ensemble-based studies have inferred much larger ΔT_{2x} values (e.g. Stainforth et al. 2005) than simulated in our study but have not reported so far the range of perturbed feedbacks strengths. The large spread of climate sensitivity in those studies implies a much larger sum of all feedbacks than discussed, e.g. by

Colman ([2003](#)), who has analysed GCMs with a ΔT_{2x} between 2.2 and 5.7°C. A larger perturbation of the individual feedbacks than covered in our study might enlarge the spread of model realizations (see Fig. [6](#)) and thus the range of inferred climate sensitivity. We account for the impact of a more extreme scanning of the realized feedback strengths by discussing the impact of structural uncertainty on our results in Section [5](#).

The parameter ranges were chosen by expert judgment (see Appendix [7.4](#)). We sampled the parameter space in a Monte Carlo manner as discussed in the subsection on sampling strategy (see above), first generating the uncorrelated ensemble, SIM_uncor, Table [1](#). This strategy yielded a range of 2.2–3.7°C for ΔT_{2x} (5–95%). Then we introduced correlations among the atmospheric parameters in order to enhance sampling of the tails of the probability distribution for ΔT_{2x} to fully span the ΔT_{2x} range covered by fully coupled GCMs (correlated ensemble, SIM_2CO2).

Using pre-industrial boundary conditions we performed 1,000 CLIMBER-2 runs in which we varied the 11 parameters simultaneously. ΔT_{2x} for each of the 1,000 model versions was calculated by running the model into equilibrium for 280 and for 560 ppm CO_2 (Table [1](#)). Together with the glacial ensembles discussed below and some additional tests, a total of about 70 million years of model simulations was performed for this study, requiring 100-cpu months on an IBM Power-4 processor (1.1 GHz).

Figure [2](#)a shows the frequency distributions of the global-mean SAT for both equilibria. The corresponding distribution of ΔT_{2x} (Fig. [2](#)b, white bars) ranges from 1.3 to 5.5°C. Figure [2](#)c shows the transient climate response (TCR), defined as the global-mean SAT increase, averaged over a 20 year period, centred at the time of CO_2 doubling (year 70 of a 1% per year CO_2 increase). This diagnostic also reflects the lag induced by ocean heat-uptake and is more directly relevant to climate change in the 21st Century than the equilibrium climate sensitivity.

Because of a broad range chosen for each of the model parameters, large discrepancies of simulated pre-industrial climate and observational data can result. Hence, we constrained the ensemble to models consistent with present-day climate. For this purpose we defined data-constraints for global characteristics of surface temperature, precipitation, sea-ice extent, volume averaged ocean temperature, as well as for Atlantic northward heat transport and North Atlantic overturning strength (see Appendix [7.2](#)). These consistency criteria reduce the original ensemble size by about 90%, which demonstrates that the parameter choices not only strongly affect the temperature response to CO_2, but also the present-day climate. However, the present-day data constraints hardly reduced the range of ΔT_{2x}. Thus the chosen parameter combinations yield a subset of model versions (Fig. [2](#), blue bars), which span a broad range of ΔT_{2x} and which all are consistent with present-day climate characteristics. This result is in line with most
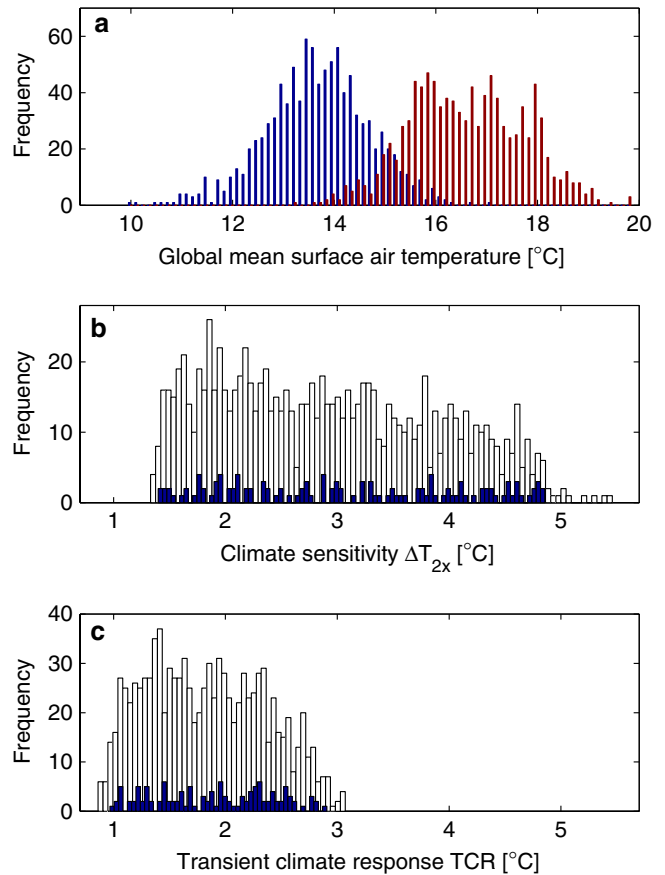

Fig. 2 Frequency distributions for pre-industrial climate characteristics (correlated ensemble, 1,000 runs). (**a**) Simulated equilibrium global-mean surface air temperature (SAT) for 280 ppm (*blue*) and 560 ppm CO_2 (*red*), corresponding distribution of (**b**), climate sensitivity ΔT_{2x}, calculated as the difference of the two equilibria, and (**c**), transient climate response (*TCR*). *Blue bars* (**b** and **c**) denote model versions consistent with present-day data. The pronounced tails (**b** and **c**) result from the chosen sampling scheme (see Section [2](#))

recent findings of GCM studies (Murphy et al. [2004](#); Stainforth et al. [2005](#)), which demonstrate that model versions with a high ΔT_{2x} cannot be ruled out by annual mean data of modern climate.

To test whether LGM proxy-data can be used to reduce uncertainty in the range of ΔT_{2x}, we then ran the full ensemble of models for LGM boundary conditions (SIM_LGM). By performing both the CO_2 doubling and the LGM experiment for each model, we automatically account for differences in feedbacks and climate response between colder and warmer climates. We do not need to assume the same sensitivity to CO_2 changes for LGM conditions as for CO_2 doubling; we thus avoid an important problem that arises in purely data-based estimates of ΔT_{2x}.

The main forcing changes between pre-industrial and LGM climate are accounted for in the simulation by lowered GHG concentrations (CO_2, CH_4, N_2O; Petit et al. [1999](#)), existence of large northern hemisphere ice sheets (Peltier [1994](#)), increased atmospheric dust con-

centration, changes in vegetation and insolation (Berger 1978). Vegetation cover is prescribed from an LGM CLIMBER-2 run with interactive vegetation scheme. Dust forcing is prescribed as top-of-the-atmosphere radiative anomalies (M. Werner, personal communication 2004, see Section 2) derived from the ECHAM-5 model (Stier et al. 2004).

For ΔT_{2x} between 2.5 and 3.5°C—a typical range for many climate models—the simulated global cooling with CLIMBER-2 (6–7.5°C) is several degrees more than that simulated in other studies (Kitoh et al. 2001; Hewitt et al. 2003; Shin et al. 2003). This systematic difference can be attributed to the combined effect of vegetation changes and dust forcing (about 1.5 to 2.0°C for the considered range of ΔT_{2x}, Schneider von Deimling et al., in preparation), which was not accounted for in the previous studies.

In order to estimate the fraction of LGM cooling attributable to lowered CO_2 concentrations, we performed two additional ensembles, in which (1) CO_2 has been lowered to its glacial value (180 ppm, implicitly accounting for CH_4 and N_2O changes) while keeping all other boundary conditions fixed to pre-industrial values (SIM_CO2_LGM, Table 1), and—to account for nonlinearities—(2) all boundary conditions have been set to LGM conditions, but CO_2 fixed to its pre-industrial value of 280 ppm (SIM_abCO2_LGM). In the latter case we calculate the contribution of CO_2 to SST cooling as the difference between this ensemble (SIM_abCO2_LGM) and the ensemble with all LGM forcings contributing to the temperature response. It can be seen (Fig. 3) that the ratio is increasing for increasing ΔT_{2x} and that (2) (green dots) yields slightly higher estimates than (1) (blue dots). In order to compare the ratio of CO_2 attributable cooling with other studies, which have neglected dust and vegetation forcing, we performed a third ensemble, which is equivalent to (1) but disregards forcing of LGM dust and vegetation changes. The resulting values for the ratio (red dots) span a range consistent with results from Shin et al. (2003) and slightly smaller than estimated by Kim (2004).

Figure 4a illustrates the simulated SAT decrease between pre-industrial and LGM climate. The ice sheet forcing maxima in the northern hemisphere are clearly reflected by the temperature response, whereas minima of LGM cooling are found in tropical regions.

Figure 4b shows the ratio of CO_2 attributable cooling (averaged over both ensembles) to total LGM cooling. The more distant from the northern hemisphere ice sheets, the larger is the relative effect of CO_2, reaching maximum values of about 50% in large areas of the southern hemisphere (Fig. 4b).

The global LGM cooling pattern looks qualitatively similar for different parameter choices, although some pronounced differences exist in well-defined regions. Figure 4c shows the standard deviation of simulated LGM cooling for all model versions consistent with present-day climate. A maximum spread of SAT decrease exists in the northern Atlantic, which can be explained by the regionally large impact of the sea-ice albedo feedback, which is strongly coupled to the location of North Atlantic convection sites (Ganopolski et al. 1998). A second, much broader maximum is found in the western Antarctic (Schneider von Deimling et al., in preparation).

Fig. 3 Fraction of LGM cooling attributable to CO_2 lowering. Shown is the ratio of annual mean LGM cooling, which is attributable to CO_2 concentration changes, to total LGM cooling for tropical SSTs (globally averaged from 30°N to 30°S). We performed two additional ensembles, in which we forced the model (1) only by LGM CO_2 changes (*blue dots*, SIM_CO2_LGM), and (2) by all glacial forcings but CO_2 (*green dots*, SIM_abCO2_LGM). The impact of vegetation and dust forcing on this ratio is illustrated by showing a third ensemble (*red dots*, equivalent to (1), but without forcing contributions from dust and vegetation)
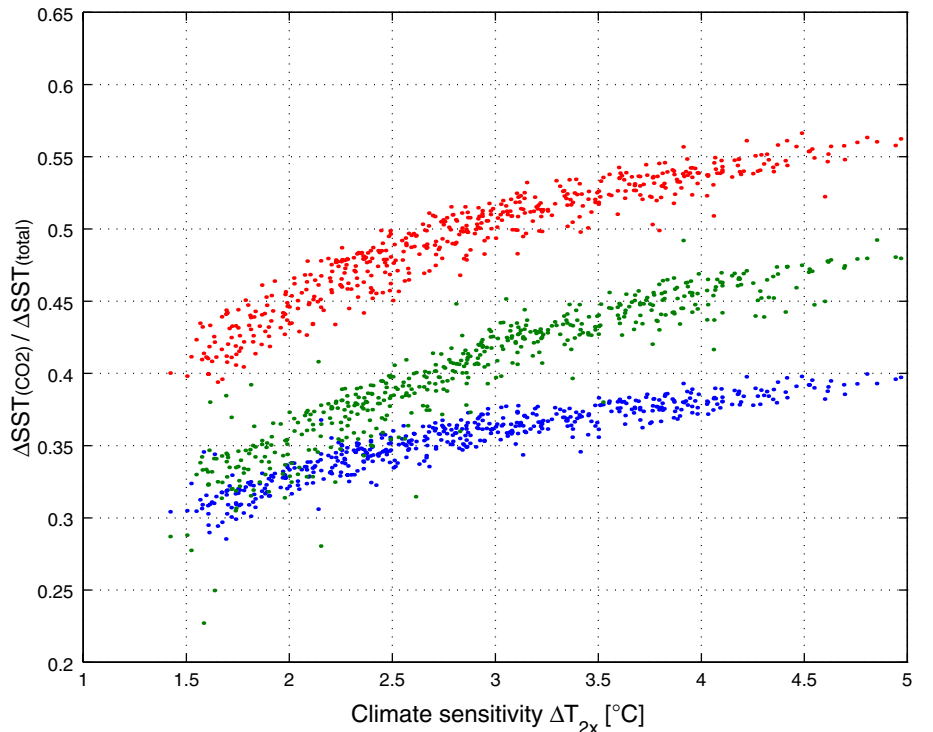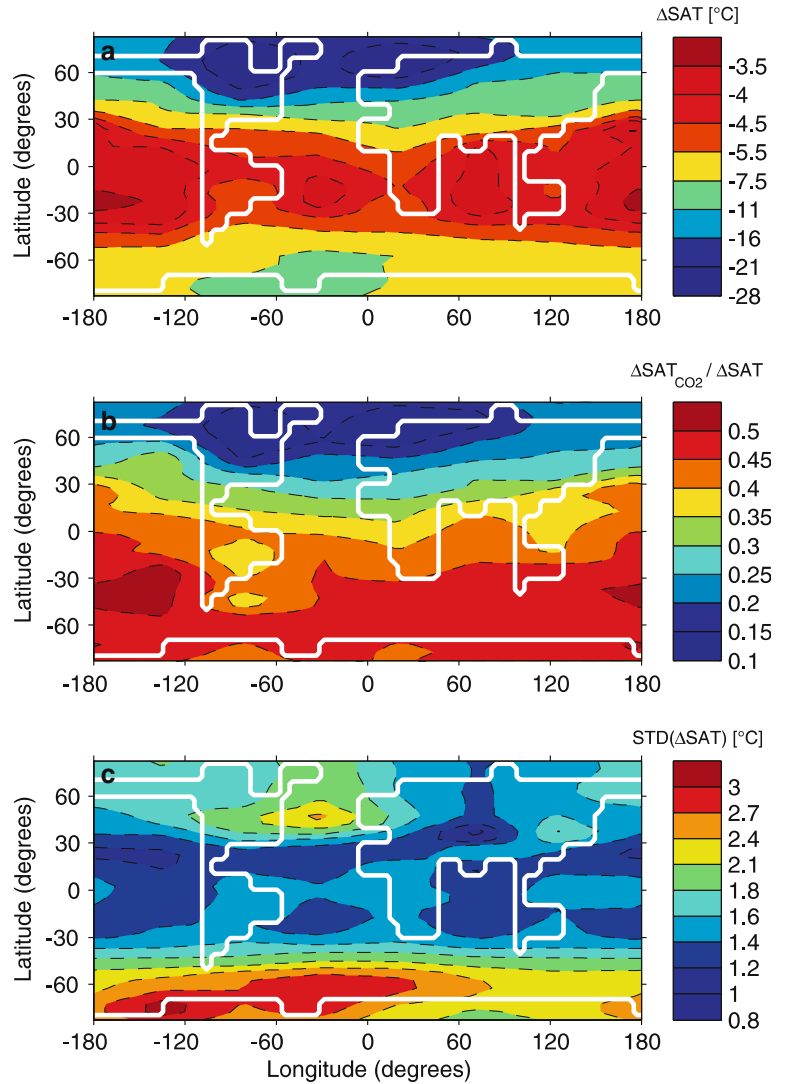
Fig. 4 Regional characteristics of LGM cooling (SIM_LGM). **a** SAT change (LGM—pre-industrial); **b** ratio of CO_2 attributable SAT cooling to total LGM SAT cooling. **a** and **b** are representative for a model version with ΔT_{2x} of 3°C, **c** shows the standard deviation of ΔSAT for all model versions consistent with present day climate

4 Constraining the climate sensitivity range

Figure 5 shows the relation between the simulated warming due to a doubling of CO_2 and the magnitude of LGM cooling for tropical and high latitude regions. The strong correlation between ΔT_{2x} and LGM cooling is striking. Model realizations consistent with present day data (blue dots) show a quasi-linear relationship between ΔT_{2x} and LGM cooling. This close link is not dependent on the exact choice of the present-day data-constraints and is the basis for our approach of constraining ΔT_{2x}. Implications of structural uncertainty and the issue of model dependence of this relation are discussed in Section 5.

When looking for the best region for applying the LGM data-constraints, several criteria have to be considered. Well-calibrated proxy data need to be available, GHGs should be an important forcing in the region, and the response should not be affected too much by regional small-scale dynamics, which cannot be resolved by our coarse-resolution model. The northern high latitudes are dominantly affected by the presence of the large continental ice sheets, with GHGs contributing only little to the signal (Fig. 4b). This makes them less suited despite the availability of Greenland ice-core data. Several Antarctic ice cores provide temperature estimates from southern high latitudes, yet covering a comparably small region of the globe. Numerous sediment-data are available from tropical ocean sites, allowing large-scale averaging over the entire tropical ocean belt (thus the importance of local processes is minimized and the relative importance of global forcings, i.e. the effect of well-mixed GHGs, is maximized). Tropical land areas are smaller and more affected by regional factors; data coverage is sparse and temperature reconstruction complicated by uncertainties of potential lapse rate changes. Hence, we chose the tropical oceans as our most reliable test region.

Reconstructed SSTs from various types of proxy-data have been discussed controversially over the past decades, particularly the magnitude of tropical tem-

perature response. Yet in recent years the analysis of different reconstruction techniques has led to reject very low and high large-scale cooling (Crowley 2000; Lea et al. 2003; Niebler et al. 2003). To derive a robust SST data constraint we use an objectively interpolated data set (Schäfer-Neth and Paul 2003), which comprises a large set of sediment cores of stringent quality and age control (about 300 for the Atlantic). We focus on data from the tropical Atlantic (20°N–20°S), which are based on GLAMAP reconstructions (Sarnthein et al. 2003), having been derived from transfer functions (TFs) of faunal assemblages of foraminifera. Accounting for reconstruction uncertainties of each data core and for uncertainty in the pattern of SST cooling, this data set yields a range of averaged tropical Atlantic SST cooling of $3.0° \pm 0.9°$ (2σ, Appendix 7.4). When considering an average over all ocean basins, slightly reduced SST anomalies would have to be applied for our analysis. A crucial issue of such an estimate is in how far the result is proxy-dependent. Geochemical SST reconstructions (Mg/Ca and alkenone methods) are in agreement with reconstructions from faunal TFs for low latitudes (Bard 2001; Rosell-Mele et al. 2004; Barker et al. 2005). Systematic differences arise in the eastern equatorial Atlantic (especially in upwelling regions), where geochemical methods (GCs) suggest a less pronounced maximum cooling (about 4°C; Rosell-Mele et al. 2004; Barker et al. 2005). We account for this possible bias by creating an alternative data set by limiting maximum tropical cooling of the original data set to 4°C, and recalculate the mean and associated error. In the following, we present results from the first set only, which yields the largest uncertainty spread (see Appendix 7.4).

To infer ΔT_{2x} from LGM data, one could go back to the unconstrained ensembles, proceed according to Bayes' formula, for both the uncorrelated as well as the correlated ensemble, and present the most extreme values for ΔT_{2x} quantiles as robust estimates. However, we would like to make use of the relations displayed in Fig. 5: a suggested linear relation between LGM cooling and ΔT_{2x}. For that we apply an "interval method" (see Appendix 7.1) that we find to be even more conservative than a Bayesian procedure, and that incorporates the information of both ensembles: we fit the linear relation from the constrained correlated ensemble as the latter is more informative in the tails of the distribution than the uncorrelated ensemble. However, we derive the error bars (for an interpretation of these error bars, see Appendix 7.1) of the linear relation from the much more scattered unconstrained ensemble. Such an evaluation is displayed in Fig. 6. Considering the error margins (5–95%) from our fitting procedure (Fig. 6) we then determine a ΔT_{2x} range, which is consistent with mean tropical Atlantic SST cooling (Appendix 7.1). The resulting range of 1.3–3.5°C (0.9–2.1°C for TCR) for our standard LGM design (SIM_LGM) is notably smaller than that estimated by the intergovernmental panel on climate change (IPCC; Houghton et al. 2001).

5 Uncertainties affecting the estimate

Our constrained ΔT_{2x} ranges crucially depend on (a) the universality of our inferred quasi-linear relationship between future warming and past cooling, thus on the model structure, (b) the applied glacial boundary conditions, and (c) the reliability of reconstructed paleo-temperatures.

Concerning (a), simulations with comprehensive climate models realized within the PMIP-2 project will be published in the near future and will help to answer the key question, whether the close correlation of LGM tropical cooling with ΔT_{2x} (Fig. 5a, b) is specific to our model, or whether it is valid more generally. A similar study with a multi-model ensemble would help to clarify the importance of processes not resolved by our model (e.g. ENSO). Physical reasoning makes a close link between mean glacial tropical cooling and ΔT_{2x} plausible. Mean glacial tropical cooling largely reflects lower CO_2 values, and is as such the inverse of an increased CO_2 experiment.

However, the shape, location and the uncertainty of such a relation (Fig. 5) depend on the model used and how or which processes are resolved or parameterised in the model. In contrast to the close linear relationship found in CLIMBER-2, Annan et al. (2005) find a much weaker correlation of glacial SST and climate sensitivity in an atmospheric GCM coupled to a slab ocean. They infer deviations of the individual simulations from a linear approximation at least five times larger than in our model. Although this may be an artifact of a slab ocean with fixed heat transport, we take this larger spread as a measure for uncertainty when using structurally different models and enlarge our inferred spread estimate by a factor of 5. The resulting upper limit of ΔT_{2x} is shifted by 1°C towards larger sensitivities. Additional to uncertainty in the spread an offset in the regression line (Fig. 6) may introduce a further bias. At this stage there are too few model realizations with fully coupled comprehensive climate models to quantify this effect. As all available PMIP-2 simulations clearly fall inside our considered uncertainty range[3] when enlarging the spread, we assume to thus account for structurally different models in a representative way.

The crucial issues for determining CO_2 sensitivity from an inverse glacial experiment are (1) what fraction of tropical glacial cooling is due to CO_2 and how much is due to other forcings and horizontal energy transport, and (2) whether there are strongly asymmetric feedbacks for warming and cooling not correctly captured by our model. Concerning (1), we have included uncertainty in aerosols, glacial ice sheets and GHG concentrations (see next section)—and we note that the horizontal energy

---

[3] For inference of consistency we compare PMIP-2 results with CLIMBER-2 simulations which are based on PMIP-2 boundary conditions (excluding forcing contributions by glacial dust and vegetation).

Fig. 5 Dependence of LGM cooling (relative to the pre-industrial climate) on ΔT_{2x} for different regions. Shown is (**a**), annual mean of average (20°N–20°S) global tropical SST cooling; and annual mean average SAT cooling for (**b**), tropical land (30°N–30°S), (**c**), Greenland, (**d**), eastern Antarctica. *Green points* represent the entire ensemble (1,000 runs, SIM_LGM), *blue points* only model versions consistent with present day climate (123 runs)
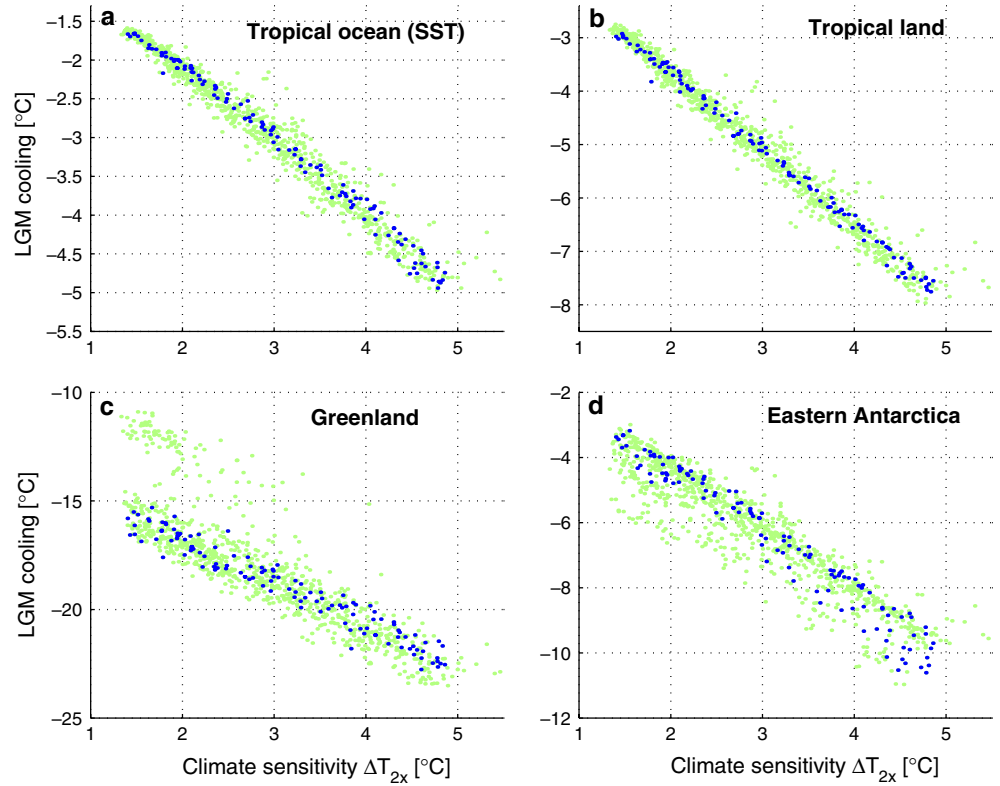
transport out of the tropics in other models is unlikely to be considerably outside the range covered in our ensemble, which yields a range of 1.4–2.0 for the ratio of global to tropical SAT cooling. Concerning (2), processes not captured by our model (e.g. ENSO-dynamics) may play a role, but this would only change our ΔT_{2x} estimate if such processes affect the mean SST of the tropics in a strongly asymmetric way for LGM and CO_2-doubling. Hence it remains open in how far a multi-model ensemble would show a much wider spread (like, e.g. seen in Annan et al. 2005) than seen in Fig. 5a. Note that derivations of ΔT_{2x} purely based on paleo-data (e.g. Lea 2004) implicitly assume a symmetry between warming and cooling and a fixed fraction of glacial cooling attributable to CO_2.

Accounting for uncertainty in the glacial forcings, we consider uncertainty in the forcing contributions of glacial dust, ice sheets and GHGs. Firstly we evaluate the impact of a possible overestimation of dust forcing in our study on ΔT_{2x} by running an identical ensemble with the dust radiative anomaly reduced by 50% (see Fig. 1). A reduction of the dust forcing by a factor of 2 leads to a small shift (about 0.3°C) of the ΔT_{2x} range to higher values. A much stronger forcing than assumed in our 100% scenario seems unlikely, or one would expect a stronger correlation between tropical SSTs and dust in the atmosphere over a complete glacial cycle.[4] Total LGM ice volume is known from sea level lowering, the maximum spatial extent of the ice sheets is well known from moraine signatures. Thus uncertainty in glacial ice

sheet forcing is mainly given by uncertainty in the shape and in the albedo of the ice sheets. We therefore reduced the standard model parameters of ice sheet albedo by 10% and derived an increase of the upper ΔT_{2x} limit of 0.5°C. The sensitivity of our results to changes in the ice sheet shape was investigated by replacing Peltier's ICE-4G ice sheet reconstruction (Peltier 1994), which we use for our standard LGM design, with ICE-5G (Peltier 2004), with most pronounced differences between the two in the Eurasian region. The difference for tropical Atlantic SST cooling between those two experiments is rather small (0.2°C, for a climate sensitivity of ~3°C). To quantify uncertainty in GHG forcing we re-run the ensemble for an *equivalent*[5] CO_2 concentration of 170 ppm, which is closer to the PMIP-2 design than our standard experiment with 180 ppm (SIM_LGM), which is more at the lower end of recent estimates of glacial–

---

[4] Ice and sediment cores indicate a drastic increase of dust deposition rate at the MIS4/MIS3 boundary (around 60 kyr BP), while SST cooling in the tropics is rather moderate at that time. Multivariate analysis of tropical SST and Antarctic dust concentration (Lea 2004) provides an upper estimate for the impact of dust on glacial temperature. Moreover, when accounting for the fact that only part of the glacial SST signal should be attributed to the increase in dust concentration and that changes in dust concentration coincide with CO_2 drop, ice sheet growth and sea level lowering, the effect of dust on LGM cooling is smaller than estimated by multivariate analysis (Lea 2004).
[5] This concentration yields the same radiative forcing as the sum of individual GHG forcings resulting from changes in CO_2, CH_4 and N_2O concentrations.

Fig. 6 Inferring ΔT_{2x} from LGM data (interval method). Simulated annual mean tropical Atlantic SST cooling (averaged from 20°N to 20°S) is shown for correlated (*blue dots*, SIM_LGM) and uncorrelated parameter ensembles (*orange dots*, SIM_uncor_LGM). The *red curve* shows the linear fit to the correlated ensemble, the *red dotted lines* represent the fit-error, conservatively estimated from the uncorrelated setting as the 5–95% of the spread of deviations from the fit. Only runs consistent with present day data are shown. *Purple* (*green*) *dashed lines* illustrate the range of ΔT_{2x} (including fit error bounds) consistent with a mean tropical Atlantic SST cooling of $3.0 \pm 0.9°C$
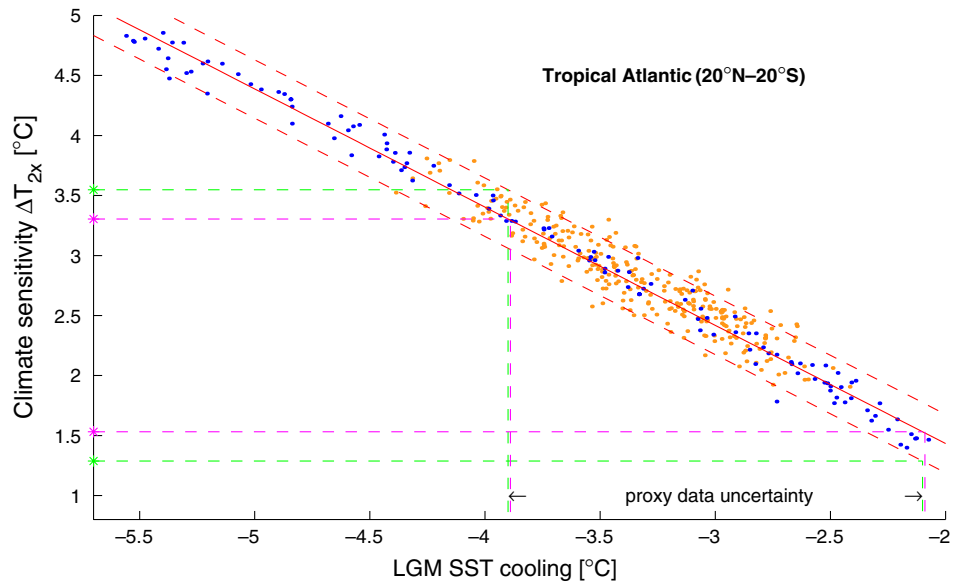
interglacial GHG concentration changes. This additional decrease of 10 ppm lowers the upper limit of ΔT_{2x} by 0.1°C.

For our further analysis we combine all considered forcing uncertainties by discussing a minimum and a maximum scenario of glacial radiative forcing (SIM_LGM and SIM_LGM0.5, see Table 1).

We assembled the effects of both scenarios in Fig. 7, by light-blue and dark-blue solid intervals, respectively.

Finally the uncertainty range of our inferred climate sensitivities depends on the reliability of the applied paleo-data. The fact that fundamentally different proxy reconstructions (such as TFs and GCs) yield consistent results for most regions of low latitudes, as, e.g. suggested by first results of a huge multi-proxy inter-com-
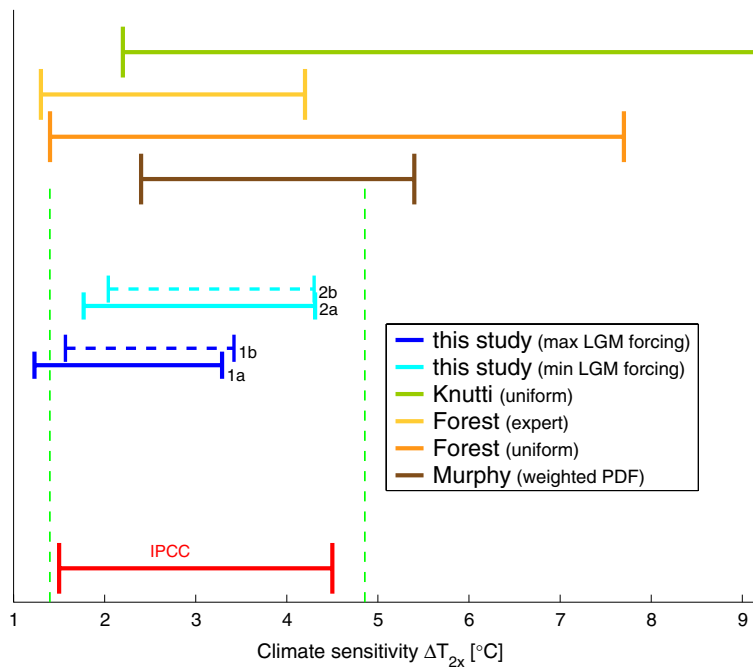

Fig. 7 Climate sensitivity estimates. The *dark* (*light*) *blue* intervals represent the 5–95% range (estimated from an interval method) of ΔT_{2x} consistent with LGM cooling for a minimum (SIM_lowRF) and maximum (SIM_highRF) assumption of glacial forcing, illustrated for mean tropical Atlantic SST cooling (3.0 ± 0.9°C, *solid lines*) and Antarctic cooling (5.4 ± 1.4°C, *dashed lines*). *Vertical green dashed lines* represent the ΔT_{2x} range resulting from the present day data consistent parameter ensemble without applying LGM constraints. Other recent ΔT_{2x} estimates [5–95%; Forest et al. 2002; Knutti et al. 2002; Murphy et al. 2004 (weighted PDF)] are shown for comparison (see legend). Note that structural uncertainty may introduce an additional uncertainty to our results yielding a maximum estimate for ΔT_{2x} of 5.3°C

parison project (Kucera et al. 2005), enhances the credibility of the considered SST paleo-temperature estimates.

When accounting for uncertainty in model parameter choices, in glacial forcings and in reconstructed paleo-temperatures, our results suggest a range for ΔT_{2x} (derived by the interval method) of 1.2–4.3°C (0.9–2.6°C for TCR). As described in more detail in Appendix 7.1, our intervals represent conservative estimates of 5–95% quantiles. Structural model uncertainty is difficult to quantify but likely to increase the inferred range. When considering a spread (discussed in Fig. 6) which is by a factor 5 larger than inferred from our results, then climate sensitivities up to about 5.3°C cannot be ruled out.

For the reasons given above, our data constraint is strongest for reconstructed tropical SSTs (based on the Atlantic). Nevertheless it is instructive to also consider other data types and regions. Tropical land data are subject to larger uncertainty (3.5–7°C cooling; Farrera et al. 1999; Pinot et al. 1999), but yield similar estimates of ΔT_{2x} (Fig. 5b). Ice-core data from Antarctica (about 5.4 ± 1.4°C cooling above the temperature inversion, and 8 ± 2°C surface cooling; Vimeux et al. 2002; Jouzel et al. 2003; Watanabe et al. 2003) constrain ΔT_{2x} independently from low latitudes, showing highly consistent results with tropical SST-based estimates (Fig. 7, note the small difference between solid and dashed blue intervals). Our model-data comparison for Eastern Antarctica is not biased by an overestimate of altitude changes in the ice sheet. We only apply changes in ice sheet altitude due to sea level lowering (120 m) for Eastern Antarctic. Comparison of ice-core temperatures from Greenland (18–20°C surface cooling; Dahl-Jensen et al. 1998) with our model simulations again yields consistent ΔT_{2x} estimates (Fig. 5c), but this should not be over-interpreted given the small size of Greenland and the coarse model resolution. Overall, the fact that very different absolute temperature changes in high and low latitudes all yield very similar estimates of ΔT_{2x} gives additional credence to our results.

6 Implications

Our results demonstrate that the tropical cooling during the LGM, as reconstructed with increasing accuracy from various types of proxy data, can provide a constraint on the upper limit of ΔT_{2x}. The effectiveness of such a constraint will crucially depend on the question how robust the link between simulated glacial cooling and future warming (ΔT_{2x}) proves to be, when an ensemble of structurally different models is considered. Simulation results from intercomparison studies (such as PMIP-2) will provide a first step towards quantifying this uncertainty. Assuming that our inferred close relationship between LGM cooling and CO_2 warming represents a universal characteristic seen as well in comprehensive climate models and assuming that the *mean* tropical Atlantic SST cooling during the LGM

(averaged from 20°N to 20°S) was in the range of 3.0 ± 0.9°C we then infer the range of consistent climate sensitivities. When additionally accounting for uncertainty in the glacial forcing our method gives a 5–95% range (conservatively estimated from an interval method; Fig. 7, solid blue intervals) of 1.2–4.3°C (up to about 5.3°C if structural uncertainties are accounted for) for the climate sensitivity to CO_2 doubling (0.9–2.6°C for the TCR).

These results are corroborated by ΔT_{2x} estimates based on reconstructed Antarctic cooling (Fig. 7, dashed blue intervals). A comparison of our inferred relationship between glacial cooling and CO_2 warming with results of comprehensive climate models (e.g. PMIP-2) will help to clarify the degree of model dependence of the exact results of our simulations. The promising outcome of this study suggests that further investigations with multi-model ensembles will be worthwhile, especially in the view of a successful first multi-thousand-member GCM ensemble (Stainforth et al. 2005), to analyse the importance of structural uncertainties for our applied methodology of constraining climate sensitivity. Progress in reducing the range of ΔT_{2x} will also come from including more regions with high-quality paleo-climatic proxy-data for the LGM (e.g. Kucera et al. 2005).

7 Appendices

7.1 Consistency criteria

For our interval method simulated climate characteristics have to lie within the ranges of all seven data-constraints to be regarded as consistent with the data (see Appendix 7.2). This prerequisite leads to an extensive rejection of parameter combinations (about 90%). Further constraints, which account for latitudinal model characteristics, have not proven to further constrain ΔT_{2x} (not shown). Application of paleo-data-constraints to this strongly constrained ensemble (123 out of 1,000 model runs) results in even fewer paleo-consistent model realizations. To derive statistically robust estimates of ΔT_{2x} we therefore approximate the inferred relationship between ΔT_{2x} and LGM SST cooling by a linear regression (Fig. 6, solid red curve). The fit uses the simulation results of the correlated ensemble (blue dots), which covers a broad range of ΔT_{2x}. We read the consistent ΔT_{2x} range from the fit-curve (pink asterisks). Then we account for the additional uncertainty on ΔT_{2x} caused by deviations from the fit.

This is realized by choosing the 5–95% of the deviation spread (represented as red dashed lines), estimated from the uncorrelated ensemble (orange dots), as it provides larger deviations than for the correlated ensemble and thus yields a more conservative uncertainty measure. Using the fit and the spread estimate, we then determine ΔT_{2x} ranges (green asterisks), which are consistent with the assumed LGM cooling.

The same methodology cannot be applied for constraining TCR, as the linear relationship between LGM cooling and equilibrium warming does not hold for the transient model response. Therefore, for TCR, we replace the linear fit by the more general function type $f(x) = a(x - x_0)^b$ (with $f \leftrightarrow$ TCR, $x \leftrightarrow$ LGM cooling) and furthermore allow the standard deviation σ of the residuals to vary with x as a quadratic function $\sigma(x)$. In fact we observe σ to mildly expand at the tails of the fit. We determine the coefficients of that function as a maximum likelihood estimate, assuming a Gaussian distribution of the residuals for each x. Both fitting procedures (the one for $f(x)$ as well as for $\sigma(x)$) are performed with the correlated ensemble that is more informative in the tails of $\sigma(x)$. However, as for the linear fitting procedure, we would like to obtain a conservative estimate in the sense that the uncorrelated ensemble displays larger values of σ. Hence we assume the same shape $\sigma(x)$ for the uncorrelated ensemble, but allow for an overall upscaling $c\sigma(x)$, c being estimated from a quadratic fit. In summary, we have generalised the linear fitting $f(x)$ including constant $\sigma(x)$ to a non-linear fit $f(x)$, $\sigma(x)$, yet ensuring that the average $\sigma(x)$ is obtained from the uncorrelated ensemble.

One may ask what would be the consequences if one applied this non-linear procedure to the estimates of ΔT_{2x} as well. We have tested for that and found only minor changes in the derived intervals. The bounds of the intervals are shifted at maximum by 0.2°C to the extremes in one case (for tropical constraints) and much less otherwise. Hence we conclude that our results derived for ΔT_{2x} are very robust against the choice of fitting curve. As a final remark on our results for TCR we would like to stress that this study is designed to constrain a characteristic of equilibrium temperature change. To effectively constrain the range of TCR, transient data information should be included in the analysis.

As a final remark on our interval method we would like to discuss its relation to a more formal procedure that would independently sample ("IS-scheme") the error distribution of the paleo-constraint and the error distribution of the fit (the latter generated from the deviation of the uncorrelated ensemble from the fit). Intervals derived from the IS-scheme could strictly be interpreted as quantiles. However, the interval transparently derived from our method is more conservative (larger) than the interval derived from the IS-scheme. In order to clarify this we would like to discuss a linear relation f (that we suppose to hold for climate sensitivity) first: there, our scheme simply adds the paleo and the fitting error, while IS would add according to Pythagoras (in the Monte Carlo scheme, the variances would add), as the paleo and the fitting error are statistically independent. Our scheme can be interpreted as choosing the worst case of perfect correlation of paleo and fitting error, leading to strictly larger error bars than the IS-scheme. As the relation f between TCR and LGM cooling is only slightly non-linear, the same statement holds for TCR as well. Finally, both schemes lead to identical results for vanishing fitting error, even for very non-linear, however, monotonous relations.

7.2 Choice of tolerable intervals for "realistic" model versions

It is still not well understood how model biases in simulation of modern climate affect climate sensitivity. Yet results from models, which produce a "realistic" modern climate state, might be preferable to "unrealistic" models. The strict and objective criteria of realistic model performance would be a requirement for model simulations to fall within the range of uncertainties of observed climate characteristics. However, even state-of-the-art climate models (GCMs) have systematic errors in simulation of different climate characteristics, which are often much larger than observations uncertainties (Covey et al. 2003). A more subjective way to assess the degree of model realism is to accept as tolerable the magnitude of errors typical for other climate models. Because this is an implicit target for any climate model development and tuning, the selection of such subjective criteria mimics a suite of models, which will be treated by other modellers as suitable for climate studies. To constrain models with empirical data we use seven global climate characteristics, which are listed below. All of these characteristics (except for the ocean temperature) have been used in SAR and TAR IPCC (Houghton et al. 1996; 2001) reports for model-data inter-comparison: we considered as tolerable the following intervals for the annual means of the following climate characteristics which encompass corresponding empirical estimates: global SAT 13.1–14.1°C (Jones et al. 1999); area of sea ice in the Northern Hemisphere 6–14 mil km^2 and in the Southern Hemisphere 6–18 mil km^2 (Cavalieri et al. 2003); total precipitation rate 2.45–3.05 mm/day (Legates 1995); maximum Atlantic northward heat transport 0.5–1.5 PW (Ganachaud and Wunsch 2003); maximum of North Atlantic meridional overturning stream function 15–25 Sv (Talley et al. 2003), volume averaged ocean temperature 3–5°C (Levitus 1982). Thus the chosen ranges—while being somewhat subjective—represent to the first approximation typical scattering of simulations with different AOGCMs (e.g. SAR and TAR IPCC reports) (Houghton et al. 1996; 2001) and encompass observational data of key present day climate characteristics.

7.3 Parameter choice

In our study the range of simulated ΔT_{2x} is affected by accounting for uncertainty in 11 model parameters, nine representing atmospheric characteristics (affecting parametrisations of cloud optical depth, height of clouds, lapse rate, tropopause height) and two describing mixing processes in the ocean. For each run all parameters have been simultaneously perturbed over the following expert derived ranges (values in {brackets} denote the standard setting for CLIMBER-2.3):

Ocean parameters: horizontal and vertical ocean diffusivity $k_H = 200$–$5,000$ {2000} m^2/s, $k_V = 0.1$–1.0×10^{-4} {0.3×10^{-4}} m^2/s at top, 1.1–2.0×10^{-4} {1.3×10^{-4}} m^2/s at ocean bottom (vertical profile after Bryan Lewis).
Optical depth of cloudiness: $ODc = (1 - Rcc) \times (OD_1 - OD_2 \times \cos(\text{latitude})^2) + Rcc \times OD_3$, with Rcc relative amount of cumulus clouds, $OD_1 = 9.0$–11.5 {10.2}, $OD_2 = 6.6$–8.4 {7.7}.
Tropopause height: $C_t = 0.74$–0.76 {0.75} (see Eq. (3) from Petoukhov et al. 2000); a further parameter ($A_{CO21} = 0.3$–0.65 {0.5}) has been perturbed, which affects the value of integral transmission function of atmosphere (D) in Eq. (3).
Lapse rate: $a_q = 625$–4440 {1,110} (kg/kg)$^{-2}$; $\Gamma_0 = 4.7$–5.2×10^{-3} {5.0×10^{-3}} K/m; $\Gamma_1 = 3.6$–4.4×10^{-5} {4.0×10^{-5}} m^{-1} (Eq. (2) of Petoukhov et al. 2000).
Height of stratiform clouds: $c_1 = 0.165$–0.200 {0.185} (Eq. (34) of Petoukhov et al. 2000).
Radiative forcing of CO_2: $A_{CO_2} = 0.70$–0.76 {0.755} (Eq. (6.7) from V. Petoukhov, A. Ganopolski, M. Claussen 2003, PIK report No. 81).

The modification of all feedback parameters results in changes of the sum of all feedbacks (water vapour, cloud, lapse rate and albedo), spanning a minimum–maximum range of 71% (63%) of the mean value for the correlated (uncorrelated) ensemble. Parameter variations, which affect the CO_2 radiative forcing, result in a range of 16% (28%) of the mean forcing.

7.4 Quantification of paleo-data uncertainties

To estimate the uncertainty range (2σ) for mean tropical SST cooling, we consider the error contributions from (a) large-scale patterns in the ocean data temperature field, which hamper a direct comparison with a coarse-resolution model, and (b) the statistical error for each reconstructed paleo-temperature value.

We refer to an interpolated data set (Schäfer-Neth and Paul 2003) from which we use the variance $V = (1.41°C)^2$ as the starting point to estimate an uncertainty range for the spatial mean of the data field. In order to do so, we need to consider the correlation structure of the individual error sources. The data were interpolated using a kriging method (Schäfer-Neth et al. 2005), which basically takes into account data points in the vicinity of a location to be reconstructed, weighted by the ocean correlation structure. This results in a spatially smoothed correlation structure of the interpolated oceanic temperature field, with only (b) being affected by the smoothing. The most extreme version of smoothing (compatible with the requirement that (a) is not affected) would result in a spatial clustering of (b) on the same scale as (a). That simplifies the discussion as then we can estimate $2\sigma \approx 2\sqrt{V/(N-1)}$, where N is given by the number of uncorrelated Atlantic ocean areas between 20°N and 20°S. With a correlation length of $\sim$10–15° we obtain a rough estimate of $N \approx 12$ for the tropical Atlantic sector. For less extreme versions of smoothing we were allowed to use larger values of N as more independent sources within (b) had entered V. In that sense $2\sigma \approx 2\sqrt{V/(N-1)}$ with $N \approx 12$ provides a conservative estimate. We thus derive an estimate of $2.96 \pm 0.85°C$ of the 2σ range for mean tropical Atlantic SST cooling.

We cannot address, however, systematic errors in paleo-temperature reconstructions beyond the quality tests of TF methods, as, e.g. described in Pflaumann et al. (2003). Reconstructed temperature anomalies from GCs agree with TF based LGM cooling estimates for most regions of low latitudes (Bard 2001; Niebler et al. 2003; Barker et al. 2005). Yet some systematic bias arises for regions of pronounced cooling (especially in the eastern tropical Atlantic). To account for this bias we confine maximum cooling in our used data set to 4°C (which corresponds to the upper limit of tropical Atlantic SST cooling derived by GC methods; Rosell-Mele et al. 2004; Barker et al. 2005). This shifts the mean about 0.2°C to less cooling and at the same time narrows the standard deviation of mean SST cooling. Thus this revised data estimate, which might be regarded as more representative for GC reconstructions, is included in the range of $2.96 \pm 0.85°C$ of our FT-based estimate and is not separately discussed for constraining ΔT_{2x}.

Given pronounced spatial inhomogeneities we emphasize that by describing mean tropical Atlantic SST anomalies, we discuss the mean annual cooling averaged from 20°N to 20°S over the whole Atlantic sector. Thus the effect of sediment cores, which show strong local effects (e.g. in upwelling regions) is minimized, and the mean SST anomaly should be more representative for large scale tropical conditions (dominated by large scale forcings, such as lowered CO_2 concentrations). Modelling and data-analysis studies show that the mean cooling for the tropical Atlantic section is slightly larger than comparable estimates from the Pacific and Indian sector. When considering a global tropical SST data-constraint, an average tropical cooling of about 2.5°C would have to be considered to constrain the same ΔT_{2x} range (as derived from tropical Atlantic).

References

Anderson TL, Charlson RJ, Schwartz SE, Knutti R, Boucher O, Rodhe H, Heintzenberg J (2003) Climate forcing by aerosol—a Hazy picture. Science 300(5622):1103–1104, DOI 10.1126/science.1084777

Andronova N, Schlesinger ME (2001) Objective estimation of the probability distribution for climate sensitivity. J Geophys Res 106:22605–22612

Annan J, Hargreaves J, Ohgaito R, Abe-Ouchi A, Emori S (2005) Efficiently constraining climate sensitivity with ensembles of paleoclimate simulations. SOLA 1:181–184, DOI 10.2151/sola.2005-047

Bard E (2001) Comparison of alkenone estimates with other paleotemperature proxies. Geochem Geophys Geosyst 2, DOI 10.1029/2000GC000050

Barker S, Cacho I, Benway H, Tachikawa K (2005) Planktonic foraminiferal Mg/Ca as a proxy for past oceanic temperatures: a methodological overview and data compilation for the Last Glacial Maximum. Q Sci Rev 24(7–9):821–834

Bauer E, Claussen M, Brovkin V, Huenerbein A (2003) Assessing climate forcings of the Earth system for the past millennium. Geophys Res Lett 30(6):1276–1279, DOI 10.1029/2002GL016639

Berger AL (1978) Long-term variation of calcoric insolation resulting from the Earth's orbital elements. Q Res 9:139–167

Berger JO (1985) Statistical decision theory and Bayesian analysis. Springer, Berlin Heidelberg New York

Broccoli AJ (2000) Tropical cooling at the last glacial maximum: an atmosphere-mixed layer ocean model simulation. J Clim 13(5):951–976

Cavalieri DJ, Parkinson CL, Vinnikov KY (2003) 30-Year satellite record reveals contrasting Arctic and Antarctic decadal sea ice variability. Geophys Res Lett 30(18), DOI 10.1029/2003GL018031

Charney JG (1979) Carbon dioxide and climate: a scientific assessment. National Academy, Washington, DC, 22 pp

Claquin T, Schulz M, Balkanski Y, Boucher O (1998) Uncertainties in assessing radiative forcing by mineral dust. Tellus B Chem Phys Meteorol 50(5):491–505, DOI 10.1034/j.1600-0889.1998.t01-2-00007.x

Claquin T, Roelandt C, Kohfeld KE, Harrison SP, Tegen I, Prentice IC, Balkanski Y, Bergametti G, Hansson M, Mahowald N, Rodhe H, Schulz M (2003) Radiative forcing of climate by ice-age atmospheric dust. Clim Dyn 20(2–3):193–202, DOI 10.1007/s00382-002-0269-1

Colman R (2003) A comparison of climate feedbacks in general circulation models. Clim Dyn 20(7–8):865–873, DOI 10.1007/s00382-003-0310-z

Covey C, Sloan LC, Hoffert MI (1996) Paleoclimate data constraints on climate sensitivity: the paleocalibration method. Clim Change 32(2):165–184

Covey C, AchutaRao KM, Cubasch U, Jones P, Lambert SJ, Mann ME, Phillips TJ, Taylor KE (2003) An overview of results from the Coupled Model Intercomparison Project. Glob Planet Change 37(1–2):103–133

Crowley TJ (2000) CLIMAP SSTs re-revisited. Clim Dyn 16(4):241–255

Dahl-Jensen D, Mosegaard K, Gundestrup N, Clow GD, Johnsen SJ, Hansen AW, Balling N (1998) Past temperatures directly from the Greenland ice sheet. Science 282(5387):268–271

Farrera I, Harrison SP, Prentice IC, Ramstein G, Guiot J, Bartlein PJ, Bonnefille R, Bush M, Cramer W, von Grafenstein U, Holmgren K, Hooghiemstra H, Hope G, Jolly D, Lauritzen SE, Ono Y, Pinot S, Stute M, Yu G (1999) Tropical climates at the Last Glacial Maximum: a new synthesis of terrestrial palaeoclimate data. I. Vegetation, lake levels and geochemistry. Clim Dyn 15(11):823–856

Forest CE, Stone PH, Sokolov AP, Allen MR, Webster MD (2002) Quantifying uncertainties in climate system properties with the use of recent climate observations. Science 295(5552):113–117

Frame DJ, Booth BBB, Kettleborough JA, Stainforth DA, Gregory JM, Collins M, Allen MR (2005) Constraining climate forecasts: the role of prior assumptions. Geophys Res Lett 32(9), L09702, DOI 10.1029/2004GL022241

Ganachaud A, Wunsch C (2003) Large-scale ocean heat and freshwater transports during the World Ocean Circulation Experiment. J Clim 16(4):696–705, DOI 10.1175/1520-0442(2003)016 < 0696:LSOHAF > 2.0.CO;2

Ganopolski A, Rahmstorf S (2001) Rapid changes of glacial climate simulated in a coupled climate model. Nature 409:153–158, DOI 10.1038/35051500

Ganopolski A, Rahmstorf S, Petoukhov V, Claussen M (1998) Simulation of modern and glacial climates with a coupled global model of intermediate complexity. Nature 391:351–356

Ganopolski A, Petoukhov V, Rahmstorf S, Brovkin V, Claussen M, Eliseev A, Kubatzki C (2001) CLIMBER-2 a climate system model of intermediate complexity. Part II. Model sensitivity. Clim Dyn 17:735–751

Gregory JM, Stouffer RJ, Raper SCB, Stott PA, Rayner NA (2002) An observationally based estimate of the climate sensitivity. J Clim 15(22):3117–3121

Hansen J, Lacis A, Ruedy R, Sato M, Wilson H (1993) How sensitive is the worlds climate. Res Explor 9(2):142–158

Harrison SP, Kohfeld KE, Roelandt C, Claquin T (2001) The role of dust in climate changes today, at the last glacial maximum and in the future. Earth Sci Rev 54(1–3):43–80

Hewitt CD, Mitchell JFB (1997) Radiative forcing and response of a GCM to ice age boundary conditions: cloud feedback and climate sensitivity. Clim Dyn 13(11):821–834

Hewitt CD, Stouffer RJ, Broccoli AJ, Mitchell JFB, Valdes PJ (2003) The effect of ocean dynamics in a coupled GCM simulation of the Last Glacial Maximum. Clim Dyn 20(2–3):203–218

Hoffert MI, Covey C (1992) Deriving global climate sensitivity from paleoclimate reconstructions. Nature 360(6404):573–576

Houghton JT et al. (2001) Climate change 2001: the scientific basis. Cambridge University Press, Cambridge p 944

Houghton JT et al. (eds) (1996) Climate change 1995: the science of climate change. Cambridge University Press, Cambridge, pp 944

IPCC WG-I (2004) Workshop on Climate Sensitivity, Paris, 26–29 July 2004

Jones PD, New M, Parker DE, Martin S, Rigor IG (1999) Surface air temperature and its changes over the past 150 years. Rev Geophys 37:173–200, DOI 10.1029/1999RG900002

Jouzel J, Vimeux F, Caillon N, Delaygue G, Hoffmann G, Masson-Delmotte V, Parrenin F (2003) Magnitude of isotope/temperature scaling for interpretation of central Antarctic ice cores. J Geophys Res Atmos 108(D12), 4361, DOI 10.1029/2002JD002677

Kim SJ (2004) The effect of atmospheric CO_2 and ice sheet topography on LGM climate. Clim Dyn 22:639–651, DOI 10.1007/s00382-004-0412-2

Kitoh A, Murakami S, Koide H (2001) A simulation of the last glacial maximum with a coupled atmosphere-ocean GCM. Geophys Res Lett 28(11):2221–2224

Knutti R, Stocker TF, Joos F, Plattner G-K (2002) Constraints on radiative forcing and future climate change from observations and climate model ensembles. Nature 416(6882):719–723

Kucera M, Rosell-Mele A, Schneider R, Waelbroeck C, Weinelt M (2005) Multiproxy approach for the reconstruction of the glacial ocean surface (MARGO). Q Sci Rev 24(7–9):813–819

Lea DW (2004) The 100 000-yr cycle in tropical SST, greenhouse forcing, and climate sensitivity. J Clim 17(11):2170–2179

Lea DW, Pak DK, Peterson LC, Hughen KA (2003) Synchroneity of tropical and high-latitude Atlantic temperatures over the last glacial termination. Science 301(5638):1361–1364

Legates DR (1995) Global and terrestrial precipitation—a comparative-assessment of existing climatologies. Int J Climatol 15(3):237–258

Lorius C, Jouzel J, Raynaud D, Hansen J, Le Treut H (1990) The ice-core record: climate sensitivity and future greenhouse warming. Nature 347:139–145

Murphy JM, Sexton DMH, Barnett DN, Jones GS, Webb MJ, Collins M, Stainforth DA (2004) Quantification of modelling uncertainties in a large ensemble of climate change simulations. Nature 430(7001):768–772

Niebler HS, Arz HW, Donner B, Mulitza S, Patzold J, Wefer G (2003) Sea surface temperatures in the equatorial and South Atlantic Ocean during the last glacial maximum (23–19 ka). Paleoceanography 18(3), DOI 10.1029/2003PA000902

Peltier WR (1994) Ice age paleotopography. Science 265:195–201

Peltier WR (2004) Global glacial isostasy and the surface of the ice-age earth: the ice-5G (VM2) model and grace. Annu Rev Earth Planet Sci 32:111–149, DOI 10.1146/annurev.earth.32.082503.144359

Petit JR, Jouzel J, Raynaud D, Barkov NI, Barnola JM, Basile I, Bender M, Chappellaz J, Davis M, Delaygue G, Delmotte M, Kotlyakov VM, Legrand M, Lipenkov VY, Lorius C, Pepin L, Ritz C, Saltzman E, Stievenard M (1999) Climate and atmospheric history of the past 420,000 years from the Vostok ice core, Antarctica. Nature 399(6735):429–436

Petoukhov V, Ganopolski A, Brovkin V, Claussen M, Eliseev A, Kubatzki C, Rahmstorf S (2000) CLIMBER-2: a climate system model of intermediate complexity. Part I. Model description and performance for present climate. Clim Dyn 16:1–17

Pflaumann U, Sarnthein M, Chapman M, d'Abreu L, Funnell B, Huels M, Kiefer T, Maslin M, Schulz H, Swallow J, van Kreveld S, Vautravers M, Vogelsang E, Weinelt M (2003) Glacial North Atlantic: sea-surface conditions reconstructed by GLAMAP 2000. Paleoceanography 18(3), 1065, DOI 10.1029/2002PA000774

Pinot S, Ramstein G, Harrison SP, Prentice IC, Guiot J, Stute M, Joussaume S (1999) Tropical paleoclimates at the Last Glacial Maximum: comparison of Paleoclimate Modeling Intercomparison Project (PMIP) simulations and paleodata. Clim Dyn 15(11):857–874

Rosell-Mele A, Bard E, Emeis KC, Grieger B, Hewitt C, Muller PJ, Schneider RR (2004) Sea surface temperature anomalies in the oceans at the LGM estimated from the alkenone-U-37(K′) index: comparison with GCMs. Geophys Res Lett 31(3), L03208, DOI 10.1029/2003GL018151

Sarnthein M, Gersonde R, Niebler S, Pflaumann U, Spielhagen R, Thiede J, Wefer G, Weinelt M (2003) Overview of Glacial Atlantic Ocean Mapping (GLAMAP 2000). Paleoceanography 18(2), 1030, DOI 10.1029/2002PA000769

Schäfer-Neth C, Paul A (2003) Gridded global LGM SST and salinity reconstruction, IGBP PAGES/World Data Center for paleoclimatology. Boulder, NOAA/NGDC Paleoclimatology Program, Boulder, CO

Schäfer-Neth C, Paul A, Mulitza S (2004) Perspectives on mapping the MARGO reconstructions by variogram analysis/kriging and objective analysis. Q Sci Rev 24:1095–1107

Shin SI, Liu Z, Otto-Bliesner B, Brady EC, Kutzbach JE, Harrison SP (2003) A simulation of the last glacial maximum climate using the NCAR-CCSM. Clim Dyn 20(2–3):127–151, DOI 10.1007/s00382-002-0260-x

Sokolik IN, Toon OB (1999) Incorporation of mineralogical composition into models of the radiative properties of mineral aerosol from UV to IR wavelengths. J Geophys Res Atmos 104(D8):9423–9444

Stainforth DA, Aina T, Christensen C, Collins M, Faull N, Frame DJ, Kettleborough JA, Knight S, Martin A, Murphy JM, Piani C, Sexton D, Smith LA, Spicer RA, Thorpe AJ, Allen MR (2005) Uncertainty in predictions of the climate response to rising levels of greenhouse gases. Nature 433(7024):403–406

Stier P, Feichter J, Kinne S, Kloster S, Vignati E, Wilson J (2004) The aerosol-climate model ECHAM5-HAM. Atmos Chem Phys Discuss 4:5551–5623

Talley LD, Reid JL, Robbins PE (2003) Data-based meridional overturning stream functions for the global ocean. J Clim 16:3213–3226, DOI 10.1175/1520-0442(2003)016 < 3213:DMOSFT > 2.0.CO;2

Vimeux F, Cuffey KM, Jouzel J (2002) New insights into Southern Hemisphere temperature changes from Vostok ice cores using deuterium excess correction. Earth Planet Sci Lett 203(3–4):829–843, DOI 10.1016/S0012-821X(02)00950-0

Walley P (1991) Statistical reasoning with imprecise probabilities. Chapman and Hall, London

Watanabe O, Jouzel J, Johnsen S, Parrenin F, Shoji H, Yoshida N (2003) Homogeneous climate variability across East Antarctica over the past three glacial cycles. Nature 422(6931):509–512, DOI 10.1038/nature01525